



## **SIMPLIFIED DRIFT-BASED FRAGILITY ASSESSMENT OF CONFINED MASONRY BUILDINGS**

J. Ruiz-García<sup>1</sup>, A. Terán-Gilmore<sup>2</sup>, and Oscar Zuñiga-Cuevas<sup>3</sup>

### **ABSTRACT**

This paper presents a simplified methodology for developing drift-based fragility curves for confined masonry (CM) buildings in seismic zones. Drift-based fragilities are derived from a stiffness-and-strength equivalent single-degree-of-freedom system subjected to a set of earthquake ground motions scaled to reach peak displacement demands associated to key damage states observed in CM buildings. It is shown that methodology is very useful for assessing the seismic vulnerability of CM structures and for estimating the earthquake-induced economic losses based on an engineering demand parameter closely related to structural damage.

### **Introduction**

Several seismic events have highlighted the vulnerability of housing dwellings in developing countries mainly those located in populated areas near the earthquake source. In Latin-America, low-cost housing dwellings and medium-rise apartment buildings have predominantly load-bearing confined-masonry walls as primary lateral-load resisting system under earthquake excitation. Confined masonry construction consists of load-bearing walls built of brick units framed by lightly-reinforced small-section reinforced concrete beams and columns. This building construction type represents a high percentage among the building population inventory in many Latin-American countries and, as a consequence, extensive damage in unreinforced and confined masonry construction has been reported after moderate to severe seismic events. Thus, tools for assessing the seismic vulnerability of CM buildings are highly desirable.

Fragility curves, which express the probability of reaching or exceeding predefined performance limit states conditioned on a ground motion intensity measure, are an essential ingredient for evaluating the seismic vulnerability of existing structures. These fragility curves can be developed from: a) expert opinion based on post-earthquake field observations, b) analytical studies of structural systems, and c) experimental results from structural components or systems. Very recently, several researchers have developed fragility curves either from analytical studies of masonry buildings (e.g. Erberik 2007, Park et al 2009) or from experimental

---

<sup>1</sup> Professor, School of Civil Engineering, Univ. Michoacana de San Nicolás de Hidalgo, Morelia 58040, México.

<sup>2</sup> Professor, Dept. of Materials, Univ. Autónoma Metropolitana, México D.F. 02200, México.

<sup>3</sup> Ph.D. Candidate, Dept. of Materials, Univ. Autónoma Metropolitana, México D.F. 02200, México.

data of masonry walls (Ruiz-Garcia and Negrete 2009) in order to evaluate the seismic vulnerability of masonry construction. Unlike the fragilities developed by Ruiz-Garcia and Negrete (2009), previous studies have employed the peak ground acceleration ((Erberik 2007, Erbay 2007) or the elastic spectral acceleration (Park et al 2009) as an intensity measure. However, there is a consensus among the earthquake engineering community, that structural damage is a consequence of lateral deformation demands imposed to the structures during earthquake ground shaking. Under this approach, fragility curves for masonry structures should be based on the level of peak displacement demand that cause selected damage states (i.e. displacement-based fragility curves).

This paper introduces a simplified methodology for developing drift-based fragility curves for confined masonry buildings representative of the Mexican construction practice. Although the methodology is general and it could be applied to masonry walls built of different types of bricks, the proposed procedure is illustrated for developing fragilities of a confined masonry building built of hand-made clay brick walls.

### **Proposed methodology**

Unlike previous investigations focused on developing fragility functions for masonry construction (e.g. Erberik 2007, Park et al 2009), the building-specific fragility functions developed in this study express the probability of being or exceeding key damage states in a particular CM building conditioned on the level of peak lateral inelastic displacement demand instead of conditioned on peak ground acceleration or pseudo-acceleration. For that purpose, the following steps are suggested: 1) for a specific building, a non-linear static analysis is performed in order to obtain their so-called capacity curve (i.e. base shear-lateral displacement curve), 2) from the capacity curve, an equivalent single-degree-of-freedom (ESDOF) system having global hysteretic features (i.e. stiffness-and-strength deterioration) is derived, 3) a series of non-linear dynamic analyses of the ESDOF system is carry out employing a set of earthquake ground motions scaled to reach the same peak inelastic displacement from the nonlinear response of the ESDOF, 4) response of the ESDOF (in terms of peak displacement demand) is statistically processed for developing a empirical fragility curve and a parametric cumulative distribution function is selected for characterizing the empirical fragility function. It should be mentioned that the target peak inelastic displacement in Step 3 should be related to displacement demand linked to specific damage states in the masonry walls. Therefore, Steps 3-4 are repeated for developing fragility curves associated to different damage states, or performance levels. Next, details for developing Steps 1-4 are explained as follows.

#### **Step 1. Nonlinear static analysis procedure for CM buildings**

In order to make possible a nonlinear static analysis of a CM building, Teran-Gilmore et al (2009) have proposed a modeling technique based on a modified version of the *wide-column* modeling strategy commonly employed by Mexican practicing engineers for the elastic analysis and design of CM buildings. According to this modeling strategy, a multi-story CM building can be idealized as bare frames (see Fig. 1a). Each wall is modeled as an equivalent column that concentrates its flexural and shear properties on its centerline. In the modified *wide-column* model, while a constant flexural stiffness is assigned to the column, the shear behavior of the

wall (including its inelastic range of behavior) is modeled through a spring located at its base having a shear force-deformation relationship defined by an appropriate backbone that describe its lateral shear force-deformation capacity. For example, Flores and Alcocer (1996) proposed a backbone curve for confined masonry walls, which is illustrated in Fig. 1b. In addition, equivalent beams having a width estimated according to the Masonry Technical Requirements of the Mexico City Building Code (MCBC 2004), are used to model the coupling effect that the slab provides to the masonry walls. Note that equivalent-end beams having infinite stiffness both for flexure and shear are used to model the part of the slab that falls within the walls' length; and that short-walls due to openings are also modeled as wide-columns.

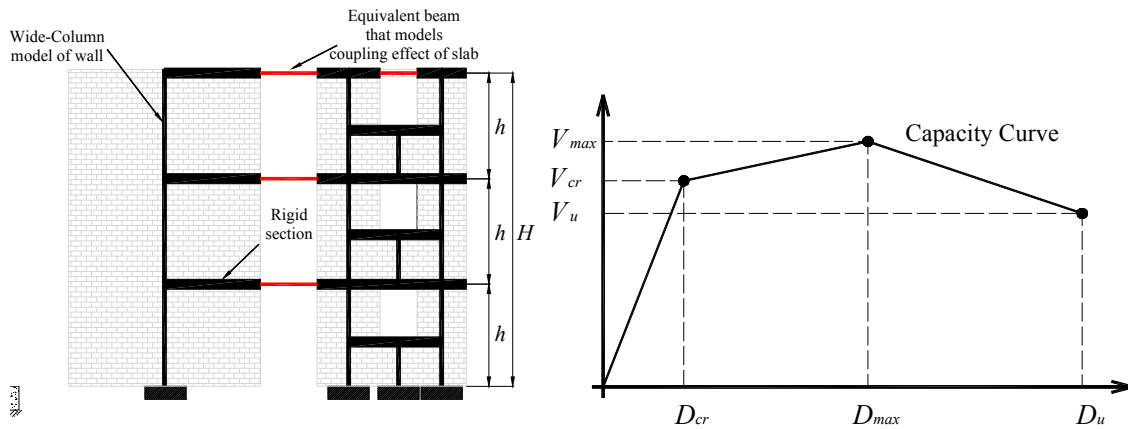


Figure 1. (a) wide-column modeling technique, (b) trilinear backbone curve for CM walls proposed by Flores and Alcocer (1996)

Figure 3 shows the modeling of full-scale two-story three-dimensional CM specimen (named specimen  $3D$ ) tested under quasi-static cyclic loading through the modified *wide-column* modeling technique implemented in the commercial software *SAP2000* (Computers and Structures Inc. 2004). In addition, the deformed shape and potential plastic hinges in specimen  $3D$  under increased lateral displacement using the Flores and Alcocer (1996) backbone curve, shown in Figure 1, is illustrated in the right side of Figure 3. It should be noted that besides providing a reasonable estimate of global behavior, the modeling technique allows for a reasonable estimation of the evolution of structural damage at the local level. This is illustrated in Figure 3b for specimen  $3D$ , which accumulated in the laboratory severe damage in the walls of the ground story and light damage in one of the walls of the upper story (Alcocer et al. 1996).

It should be noted that the modified wide-column modeling technique described above was calibrated using the experimental capacity curve of a 1:2 scale three-story hand-made clay-brick confined masonry building tested at a shaking table testing facility (Teran-Gilmore et al. 2009). It was found that the wide-modeling technique slightly overestimated the initial stiffness, it predicted very well the base shear associated to the first cracking in the first-story walls, and under predicted the maximum base shear capacity. However, the lateral displacement that according to the experimental evidence is associated to the maximum lateral strength of the building had a close correspondence with its analytical counterpart.

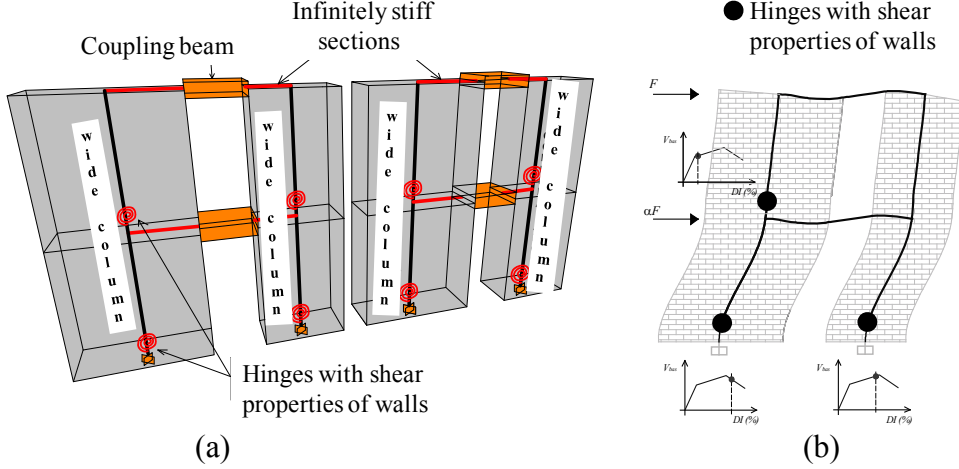


Figure 2. (a) Modified wide-column modeling technique for static nonlinear analysis, (b) deformed shape and potential plastic hinges in Specimen 3D.

## Step 2. Degrading equivalent single-degree-of-freedom system

From the global CM building-specific capacity curve,  $\mathbf{V} - \delta$ , it is possible to establish the capacity curve of an equivalent single-degree-of-freedom system (ESDOF), in the spectral acceleration-spectral displacement space,  $\mathbf{S}_a - \mathbf{S}_d$ . The following equations can be employed for such a transformation:

$$\mathbf{S}_a = \mathbf{V} / \alpha_j W \quad (1)$$

$$\mathbf{S}_d = \delta / PF_{ij} \quad (2)$$

where  $\alpha_j$  is the modal participation factor for the base shear at mode  $j$  and  $PF_{ij}$  is the modal participation factor for story  $i$  at mode  $j$ , which can be computed as follows:

$$PF_{ij} = [\sum_{k=1}^N m_k \phi_{kj} / \sum_{k=1}^N m_k \phi_{kj}^2] \phi_{ij} \quad (3)$$

$$\alpha_j = [\sum_{k=1}^N m_k \phi_{kj} / [\sum_{k=1}^N m_k] \sum_{k=1}^N m_k \phi_{kj}^2] \quad (4)$$

where  $N$  is the number of stories,  $m_k$  is the mass associated to story  $k$

Experimental evidence from full-scale isolated confined masonry walls and a full-scale three-dimensional two-story confined masonry specimen (Alcocer et al. 1996) tested under cyclic lateral loading during research programs carried out in Mexico have shown that confined masonry structures exhibit structural degradation hysteretic features (i.e. stiffness degradation, strength deterioration, and pinching). In this investigation, an enhanced version of the well-known three-parameter model (Kunnath 2003) was used in order to capture the global force-deformation response of confined masonry structures. The analytical model is able to simulate several types of hysteretic behavior through an adequate selection of parameters that control the rate of stiffness degradation, strength deterioration and pinching, which are functions of the displacement ductility reached in previous cycles and the cumulative dissipated hysteretic

energy. Thus, the parameters were calibrated using the force-deformation data obtained from a full-scale three-dimensional two-story confined masonry specimen, named specimen 3D, tested under alternate lateral cyclic loading controlled by a displacement-based protocol (Alcocer et al 1996). The experimental and simulated hysteretic response of specimen 3D is shown in Figs. 3a and 3b. As it can be seen, the analytical response is in good agreement with respect to the experimental response.

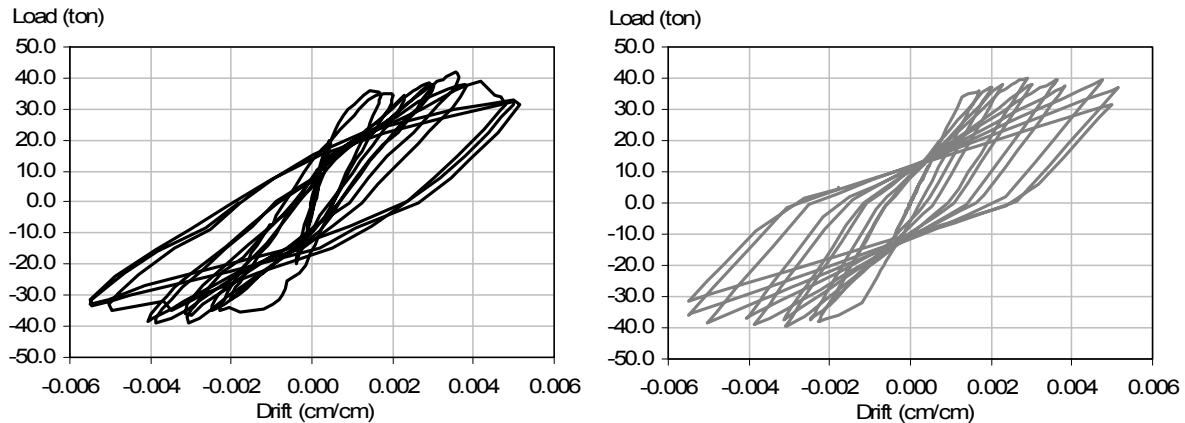


Figure 3. Hysteretic response simulation of specimen 3D: a) Experimental response; b) analytical response simulation.

### Step 3. Ground motion scaling procedure to reach different damage states

The following step requires the nonlinear response of the ESDOF system when subjected to a set of earthquake ground motions representative of the seismic hazard environment. It is proposed to scale each record to trigger the same peak displacement demand in the ESDOF, which can be associated to specific damage states in the masonry walls (e.g. peak displacement associated to the first diagonal cracking or peak displacement associated to appearance of X-shape diagonal cracking). Recently, rigorous and simplified procedures have been proposed for computing hazard curves of peak displacement demand and, furthermore recent studies have shown that this scaling procedure leads to smaller record-to-record variability than scaling earthquake ground motions to the same spectral acceleration or the same peak ground acceleration, particularly for evaluating residual displacement demands (Ruiz-Garcia and Miranda 2010).

In this investigation, three key damage states for confined masonry walls were identified based on the damage patterns observed in laboratory tests and post-earthquake field reconnaissance (see Figure 4):

- Damage State 1 (**DS<sub>1</sub>**). This corresponds to the beginning of diagonal cracking, usually smaller than 0.1 mm, on the wall surface.
- Damage State 2 (**DS<sub>2</sub>**). This damage state is characterized by fully-formed X-shaped cracking on the wall surface, of about 5 mm, concrete crushing at the bottom of tie-end columns, and horizontal hairline cracking spread along the height of the tie-end columns. This damage state is usually observed when the specimen reaches its maximum lateral load capacity at any loading direction.
- Damage State 3 (**DS<sub>3</sub>**). This damage state corresponds to the ultimate capacity of the CM walls.

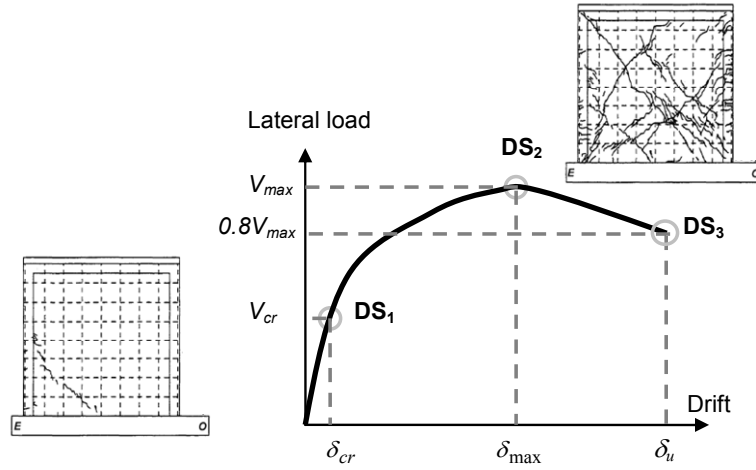


Figure 4. Damage states identified in CM walls considered in this study.

Based on a drift-based fragility study developed by Ruiz-García and Negrete (2009), damage states 1 and 2 are associated to inter-story drift ratios of 0.09% and 0.31%, respectively. In spite of the high scatter, an inter-story drift ratio of 0.5% was assumed for damage state 3.

#### Step 4. Development of drift-based fragility curves

For each intensity measure corresponding to each damage state, the empirical cumulative distribution of **IDR** was obtained by considering peak drift values of the ESDOF as independent outcomes. Sample data was then sorted in ascending order and plotted with a probability equal to  $i/n + 1$  where  $i$  is the position of the drift ratio and  $n$  is the size of the sample. From the empirical cumulative distribution, a parametric lognormal distribution is employed for defining drift-based fragilities associated to each damage state as follows:

$$P[DS > ds_i | IM = IDR] = 1 - \Phi[\ln(IDR) - \mu_{\ln IDR} / \beta] \quad (5)$$

where  $P[DS > ds_i | IM = IDR]$  is the conditional probability of reaching or exceeding damage state  $i$  in the CM structure,  $ds_i$ , at a target inter-story drift value,  $IDR$ , while  $\Phi$  is the standard normal cumulative distribution. In this investigation, the central tendency parameter was computed from the geometric mean of the data. The dispersion parameter  $\beta$  represents the total variability, which should include both the aleatory and epistemic uncertainty that arises from the seismic demand and the structural capacity. However, it should be noted that this study only included the record-to-record variability (i.e. aleatory uncertainty) as a source of uncertainty.

#### Illustrative example

The proposed simplified drift-based fragility assessment procedure for confined masonry (CM) buildings is illustrated using a four-story CM building made of hand-made solid clay bricks and designed to satisfy the Masonry Technical Requirements of the 2004 Mexico City Building Code (MCBC, 2004) having a total weight of 298 000 kg. Structural layout of the study-case CM building is shown in Fig. 5.

Under the assumption that the CM building did not experience previous structural damage, Table 1 reports dynamic properties of the study building corresponding to the first-mode shape and the first story. Employing the modeling technique described in this paper, while the capacity curve for the first floor is shown in Fig. 7, the corresponding capacity curve in the  $S_u - S_d$  space is shown in Fig. 8. From this capacity curve, the stiffness-and-strength ESDF system is derived having a yield strength coefficient equal to 0.298.

Table 1. Dynamic properties for developing the ESDOF system of the study-building

$T_1(\text{sec})$	$\phi_{1j}$	$PF_{1j}$	$\alpha_1$	$C_y$
0.233	0.0749	0.387	0.8796	0.298
	0.1437			
	0.2005			
	0.2400			

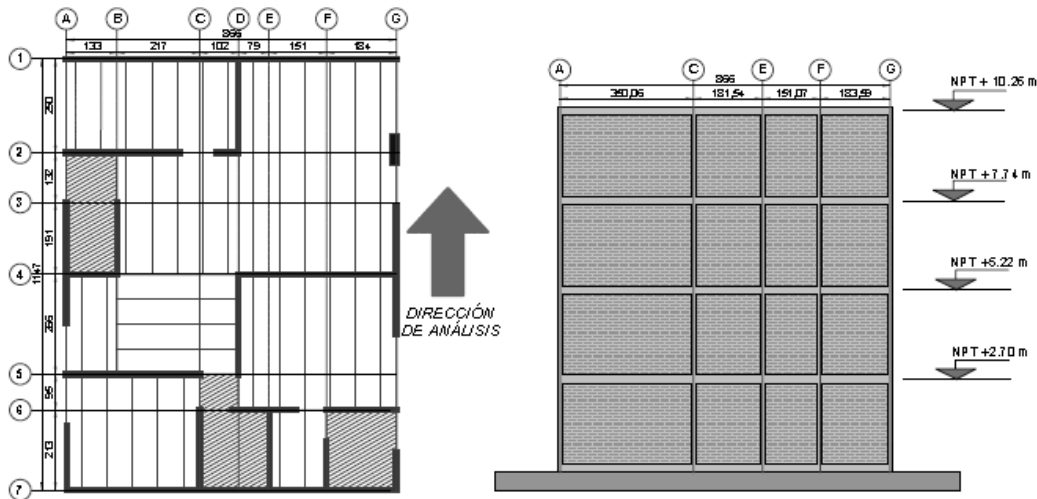


Figure 5. Structural layout of the test four-story CM building built of hand-made clay-brick.

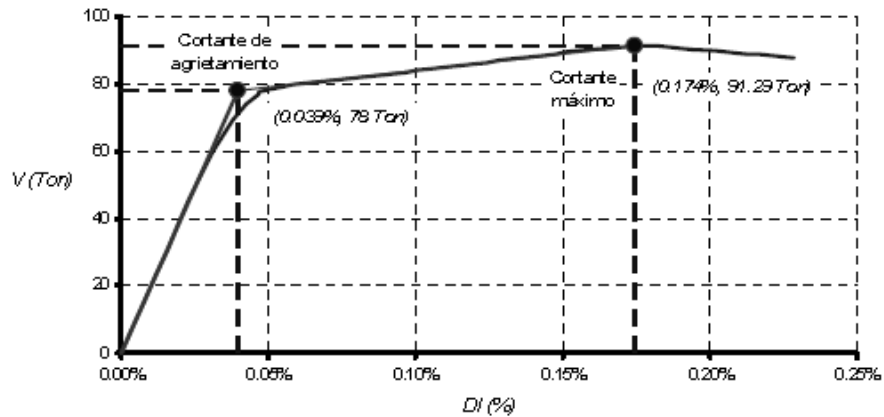


Figure 6. Capacity curve obtained for the first floor of the test CM building.

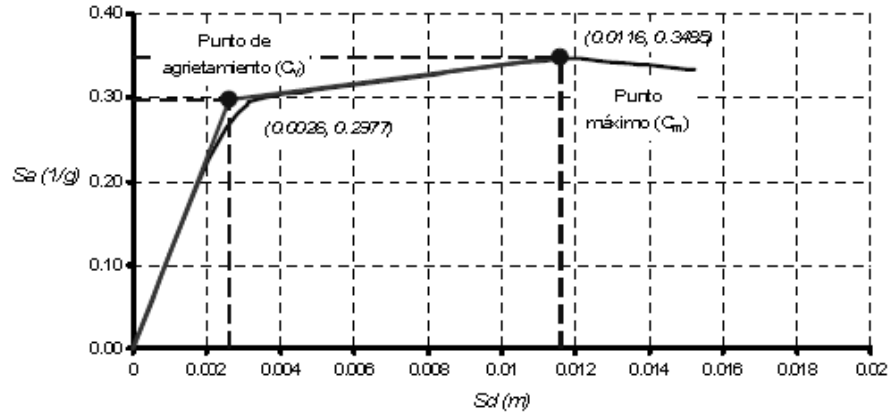


Figure 7. Capacity curve in the spectral acceleration-displacement space for the first floor of the test CM building.

In order to develop drift-based fragility curves for the test CM building, an ensemble of 24 earthquake ground motions recorded during four historical earthquakes, having surface-wave magnitude range between 5.4 and 8, on free-field stations placed on firm soil sites and located in front of the subduction zone of the Mexican Pacific Coast, including acceleration time histories from the Michoacan 1985 earthquake ( $M_s = 8.1$ ), was considered in this investigation. It is believed that this ground motion ensemble is representative of the seismic environment that threatens typical masonry construction in Mexico since recordings stations are located near the regions where structural damage to confined masonry structures has been observed during post-earthquake field reconnaissance. The elastic acceleration spectra,  $S_a$ , computed from the ground motion database is shown in Fig. 8. It can be seen that building's fundamental period of vibration is close to the peak median spectral acceleration (416.6  $\text{cm/s}^2$ ).

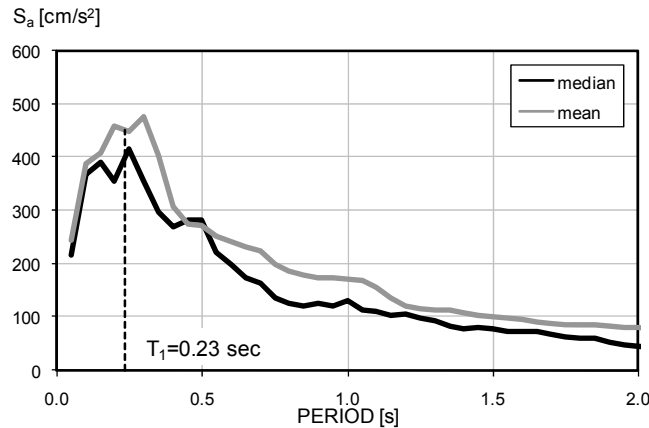


Figure 8. Central tendency of elastic spectral acceleration spectra corresponding to the set of 24 earthquake ground motions considered in this study.

Next, each earthquake ground motion was scaled to reach peak displacement demand associated to target inter-story drift ratios,  $IDR_{target}$ , of 0.09%, 0.30% and 0.50%. Then, nonlinear time-history analysis of the ESDOF system under each scaled ground motion was performed. Fig. 9 shows the distribution of peak displacement demand of the stiffness-and-strength degrading ESDOF system under each intensity level.



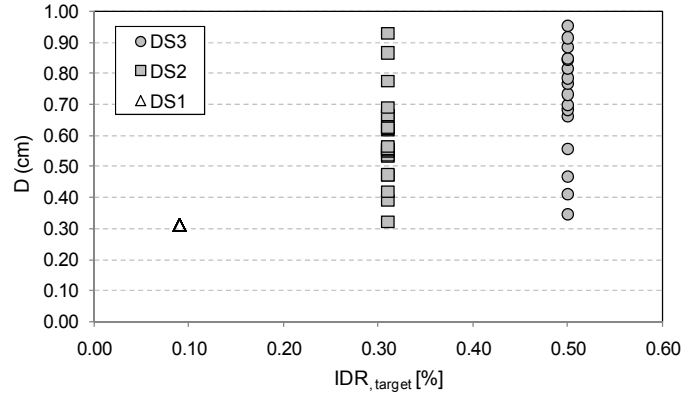


Figure 9. Distribution of peak displacement demand corresponding to three ground motion intensities.

Following the procedure described in the previous section, empirical and parametric drift-based fragilities were obtained for each damage state as shown in Fig. 10. It can be seen that the record-to-record variability increases as the ground motion intensity increases, which is reflected in the fragilities. As an example, for the test CM building under this set of ground motions, it can be seen that while there is an 81% chance of reaching **DS<sub>2</sub>**, there is about 44% chance of reaching **DS<sub>3</sub>** in the first floor for an inter-story drift ratio of 0.3%. An estimation of the peak inter-story drift demand in CM buildings can be obtained from the methods proposed by Terán et al. (2009) as well as Ruiz-García and Negrete (2009).

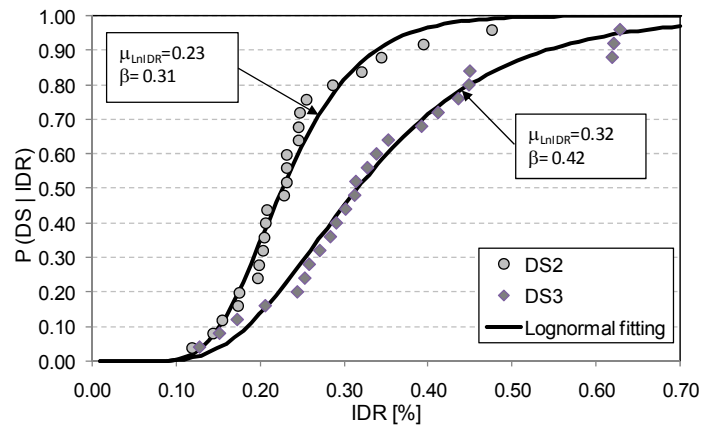


Figure 10. Drift-based fragility curves developed for the four-story CM test structure.

## Conclusions

A procedure for developing drift-based fragility curves to be used during the seismic assessment procedure of existing low-to-medium rise confined masonry buildings was presented in this paper. The methodology employs a recently proposed modeling technique for carrying out a nonlinear static analysis of confined masonry buildings, whose prevalent failure mode is associated to the CM wall's shear failure, to obtain the so-called capacity curve as well as a stiffness-and-strength degrading equivalent single-degree-of-freedom (ESDOF) system. Unlike alternative methodologies, the proposed procedure allows estimating the fragilities based on the peak inter-story drift demand, which is an engineering demand parameter closely related to structural damage.

## Acknowledgments

While the first author would like to express his gratitude to *Universidad Michoacana de San Nicolás de Hidalgo*, the second author is grateful to *Universidad Autónoma Metropolitana* in Mexico for the support provided to develop the research reported in this paper.

## References

Alcocer, S.A., Ruiz, J., Pineda, J., and J.A. Zepeda, 1996. Retrofitting of confined masonry walls with wire-welded mesh, Proceedings of the Eleventh World Conference on Earthquake Engineering, Acapulco; Paper No. 1471.

Computers and Structures, Inc. (2004). SAP2000 Advanced 9.0.3, Berkeley, California.

Erberik, M.A., 2007. Generation of fragility curves for Turkish masonry buildings considering in-plane failure modes, *Earthquake Engrg. Struct. Dyn.* 37(3), 387-405.

Flores, L.E. and S.M. Alcocer, 1996. Calculated response of confined masonry structures, in Proceedings of the Eleventh World Conference on Earthquake Engineering, Acapulco; Paper No. 1830.

Kunnath, S. K., 2003. IDASS. Inelastic Dynamic Analysis of Structural Systems, Version 3.01, University of California at Davis, CA.

Mexico City Building Code (MCBC), 2004. Normas Técnicas Complementarias para Diseño y Construcción de Estructuras de Mampostería. Gaceta oficial, Gobierno del Distrito Federal (in Spanish).

Park, J., Towashiraporn, P., Craig, J.E., and B.J. Goodno, 2009. Seismic fragility analysis of low-rise unreinforced masonry structures, *Engineering Structures* 31, 125-137.

Ruiz-García, J., and E. Miranda, 2010. Probabilistic estimation of residual drift demands for seismic assessment of multi-story framed buildings, to appear in: *Engineering Structures* 32.

Ruiz-García, J., and M. Negrete, 2009. Drift-based fragility assessment of confined masonry walls in seismic regions, *Engineering Structures* 31, 125-137.

Ruiz-García, J., and M. Negrete, 2009. A simplified drift-based assessment procedure for regular confined masonry buildings in seismic regions, *J. of Earth. Engrg.*, 13:4,520-539.

Ruiz-García, J., and E. Miranda, 2007. Probabilistic estimation of maximum inelastic displacement demands for performance-based design, *Earth. Engrg. & Struct. Dyn.* 36(9), 1237–1258.

Teran-Gilmore, A., Zuñiga-Cuevas, O., and J. Ruiz-García, 2009. Displacement-based seismic assessment of low-height confined masonry buildings, *Earthquake Spectra* 25(2), 439–464.